Draft version December 31, 2023
Typeset using LaTeX **twocolumn** style in AASTeX631

The Spectra of Carbon and Wolf-Rayet Stars Revealed by DoA Dome Telescope

Jin Bingcheng[1]

[1]*Department of Astronomy, School of Physics, Peking University, Beijing 100871, China*

ABSTRACT

I present the data reduction process and final results for DoA Dome Telescope spectroscopic observations for several carbon stars and Wolf-Rayet stars. These data consist of slitless spectra over all pointings. I reduced the spectroscopic data with a self-bulit Calibration Pipeline, with custom modifications and reduction steps designed to address additional features and challenges with the data. Here I provide a detailed description of each step in my reduction and a discussion of final measurement results. The final results are spectra for carbon stars and Wolf-Rayet stars, and I will point out features in the spectra and compare them with previous measurements.

Keywords: Spectroscopy, carbon star, Wolf-Rayet star, Wavelength Calibration, Flux Calibration

1. INTRODUCTION

In November 2023, the class OBS 2023 used DoA Dome telescope to observe several carbon stars and Wolf-Rayet stars. The observing schedule includes Carbon stars WZ Cas, HK Lyr, Wolf-Rayet stars V1687 Cyg, HD 16523, and calibration stars HIP 90191, HIP 117371. The scientific goal of this observation is to measure the spectral energy distribution of these stars with typical emission lines. To achieve this goal, My report is structured as follows. In Section 2, I will describe the observation and data acquisition. In Section 3, I present my own data reduction process, which is a custom pipeline for spectrum reduction, quite different from the image reduction pipeline. In Section 4, I will point out the known issues in the data reduction. In Section 5, the final results is presented, and I will discuss the features in the spectra and compare them with previous measurements.

2. DOA DOME TELESCOPE OBSERVATIONS

The DoA Dome Telescope is a 40cm telescope located at DoA Dome Observatory in Peking University, Beijing, China. The detector is a 36mm×24mm QHY-11 CCD with 9um pixels, giving a field of view of approaximately 30×20 square arcmins. The data consist of slitless spectroscopy over all pointings. For different star observations, we have multiple exposures for each sources. The observation log is shown in Appendix 1.

3. IMAGE REDUCTION

3.1. *Stage1 – Detector-level Corrections*

Stage 1 of my Calibration Pipeline performs detector-level corrections, many of which are common to all instruments and observing modes. This stage of reduction take care of instrumental contaminations on the CCD chip, including bias, dark, and flat field corrections.

3.1.1. *Bias Subtraction*

For every single image taken by the CCD, there is a bias level that is added to the image. This bias level is a result of the CCD electronics and is independent of the exposure time (might be influenced by the temperature of the electronics). The bias level is measured by taking a zero-length exposure, which is an exposure with zero exposure time. The bias level is then subtracted from every image taken by the CCD. This step is actually done by Professor Wang Ran, and I just use the bias subtracted images in the following steps.

3.1.2. *Dark Subtraction*

Dark subtraction is a process that removes the dark current from the CCD. The dark current is a result of thermal electrons in the CCD that are generated by the heat of the CCD. The dark current is measured by taking a series of exposures with the same exposure time as the science images, but with the shutter closed. This step is again done by Professor Wang Ran, and I just use the dark images and average them into a single dark image for each exposure time to subtract the dark current from the science images.

3.1.3. *Flat Correction*

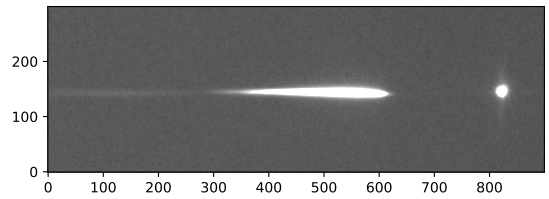

Figure 1. Trimmed image. The 0 order diffraction is on the right side of the image.

Flat correction is a process that corrects for pixel-to-pixel sensitivity variations across the CCD. The flat correction is performed by dividing each image by a normalized flat field image. Again here, the flat field image is provided by Professor Wang Ran, with dark and bias subtracted. The flat field image is normalized by dividing the median value of the image. The science images are then divided by the normalized flat field image, directly after the dark subtraction step.

3.2. *Stage2 – Individual Image Calibration*

Stage 2 of my Calibration Pipeline performs calibrations that are specific to individual images. These calibrations are performed on each image independently of all other images.

3.2.1. *Image Alignment*

Though there are too few stars in individual images to calibrate the astrometry, I still need to align the images to a common reference frame. This is because the images are not perfectly aligned due to the telescope tracking error. The alignment is performed by using the scikit-image package[1], which is capable of translating images with sub-pixel accuracy.

After careful alignment, I am able to combine 'dithered' images into a single SNR improved image. The reason I use the phrase 'dithered' is because the images are not dithered intentionally, but the telescope is not tracking the target perfectly, so the images are dithered unintentionally, which, however, is good for combining images when there are defects in the detector. For spectroscopic observation, since the dispersion is always traced in the middle of the detector, where the detector is most sensitive, I choose to combine the images by simply stacking them together.

3.2.2. *Rotation*

The images are rotated by a certain degrees, because the dispersion is not perfectly parallel to the detector.

[1] https://scikit-image.org/

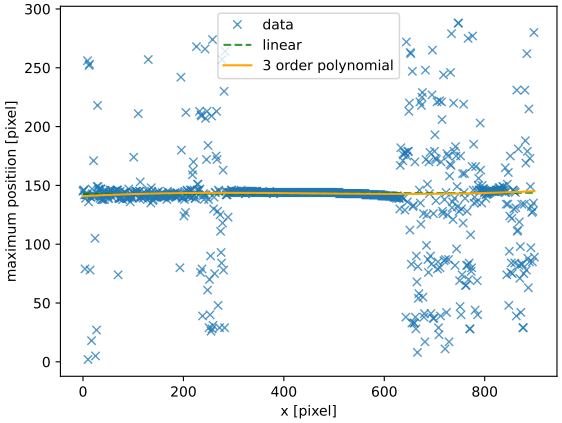

Figure 2. Traced profile. The profile is best characterized by a 3rd order polynomial function.

This will introduce a convolutional effect when extracting the spectrum, where the light from nearby wavelength will be mixed together, smoothing the whole spectrum. To avoid this effect, I rotate the images so that the dispersion is parallel to the detector. The rotation is performed by scikit-image package again. This step is checked by the traced profile in the following section 3.3.1.

3.2.3. *Trimming*

The images are trimmed to remove regions that are not needed, in order to reduce the size of the image, avoiding unnecessary computation. The images are trimmed to a size of 900×300 pixels, which covers both the 0 order diffraction and the dispersed light in optical band, shown in Figure 1.

3.3. *Stage3 – Science-level Calibration*

Stage 3 of my Calibration Pipeline performs science-level calibrations to images. These calibrations are performed on all available images together, and are therefore able to take advantage of the statistical properties of the ensemble.

3.3.1. *Extracting Spectrum*

The spectrum is extracted by first tracing the profile, which is the intensity of the light along the dispersion direction. The profile is traced by the maximum intensity of the light along the dispersion. The profile is then fitted by a low order polynomial function, which is shown in Figure 2.

The aperture size is chosen to be 7 pixels, then the spectrum is extracted by summing the intensity of the light within the aperture along the dispersion axis. To

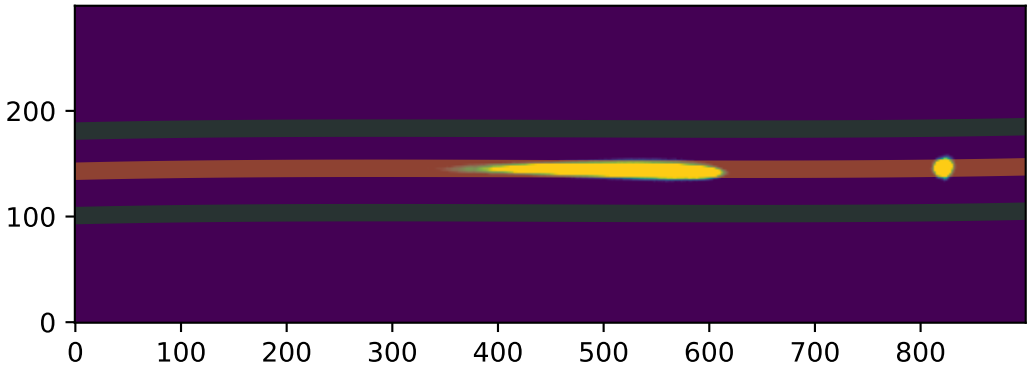

Figure 3. Aperture and background regions. The aperture is chosen to be 7 pixels, and the background regions are 7 pixels wide each side.

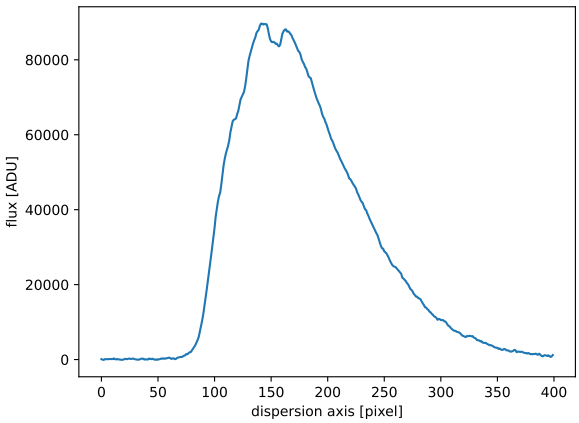

Figure 4. Uncalibrated 1D spectrum. The spectrum is extracted by summing the intensity of the light within the aperture along the dispersion axis.

estimate background, I use two regions on both sides of the aperture, which is shown in Figure 3.

The background is estimated by the mean value of the intensity in the two regions. The 1D uncalibrated spectrum is finally obtained by subtracting the background from the aperture sum, shown in Figure 4.

3.3.2. *Wavelength Calibration*

Wavelength calibration is a process that converts the pixel position of sources in the image to the wavelength of the light from the source.

I use the hydrogen Balmer series as the reference because our choice of calibration star, an A0IV type star, has strong feature of hydrogen Balmer series absorption lines, mostly Hβ and Hγ. The wavelength calibration is performed by fitting the pixel position of the hydrogen Balmer series absorption lines to the wavelength of the lines. The 0 order of the diffraction is fitted by an 1D gaussian function using the astropy package[2], which is the zeropoint of the wavelength calibration. Figure 5 shows the wavelength calibration result. The dispersion is 17.75Å/pixel, which is consistent with the value of 17.5 Å/pixel given by star analyser 200. More importantly, the calibrated wavelength of typical absorptions or emissions are consistent with the literature values, as shown in Section 5, which indicates that my wavelength calibration is reliable.

Though the result seems reliable, there could be a problem with the location of Balmer series. This will be discussed in Section 4.2.

The specutils package[3] helps to assign the calibrated wavelength to the uncalibrated 1D spectrum, which is shown in Figure 6. To do this, I still need a gaussian function to fit the 0 order of the diffraction.

3.3.3. *Flux Calibration*

Flux calibration is a process that converts ADU (Analog-to-Digital Unit) to physical flux. The flux calibration is performed by using the standard SED of the calibration star. The standard SED is provided by professor Wang Ran, which is shown in Figure 7. Since the spectral resolution of the DoA Dome Telescope is not high enough to resolve most features in the standard SED, the flux calibration is performed by fitting the smoothed standard SED to the observed spectrum. The product of the fitting is the sensitivity function, which is not only determined by the detector response, but also the atmospheric transmission and the telescope

[2] https://www.astropy.org/

[3] https://specutils.readthedocs.io/en/stable/

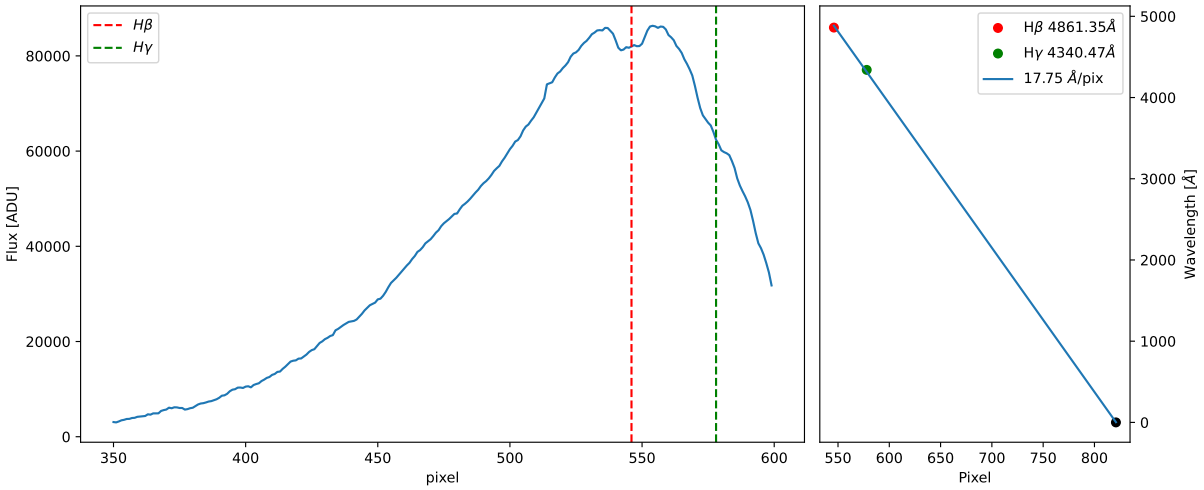

Figure 5. Wavelength calibration. The 0 order of the diffraction is fitted by an 1D gaussian function using the astropy package. The pixel position of the hydrogen Balmer series absorption lines are fitted to the wavelength of the lines.

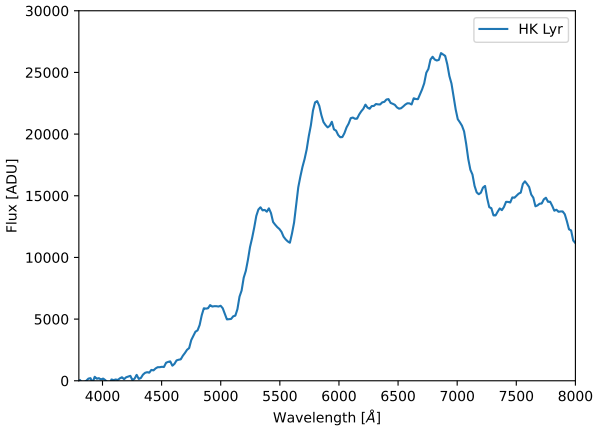

Figure 6. Wavelength calibrated 1D spectrum. The specutils package helps assign the calibrated wavelength to the uncalibrated 1D spectrum.

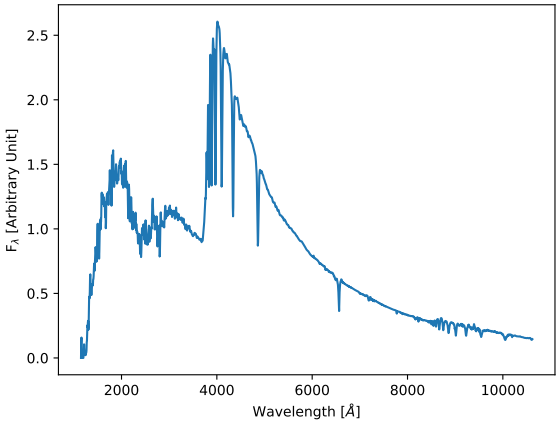

Figure 7. Standard SED of the calibration star HIP 90191, an A0IV type star. The standard SED is provided by professor Wang Ran.

transmission. The sensitivity function is shown in Figure 8.

The sensitivity function is then used to convert the wavelength calibrated 1D spectrum to the final 1D spectrum, shown in Figure 9. In order to preserve most of the information from the sensitivity function, rather than fitting a polynomial function, I interpolate the sensitivity function to the wavelength grids of the observed spectrum. The interpolation is performed by the specutils package.

4. KNOWN ISSUES

4.1. *Error Budget*

The error of spectra cannot be calculated directly from the science data. I need to construct an error map for science image with not only science frame itself, but flat frame, dark frame and bias frame as well. However, since I cannot obtain the readnoise from the detector, it's hard to only construct the error map with the poisson noise. And the error will propogate during the calibration process including stacking.

4.2. *Location of Balmer Series*

There could be a problem with the location of Balmer series, as I only recognize them by eye in Figure 6. The location of Balmer series is important for wavelength calibration, especially in the case where only Hβ and Hγ are available. The systematic error of the wavelength calibration will be large if the location of Balmer series is

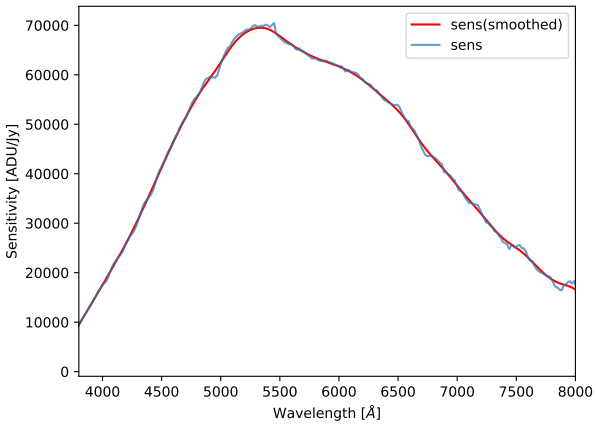

Figure 8. Sensitivity function. The sensitivity function is not only determined by the detector response, but also the atmospheric transmission and the telescope transmission.

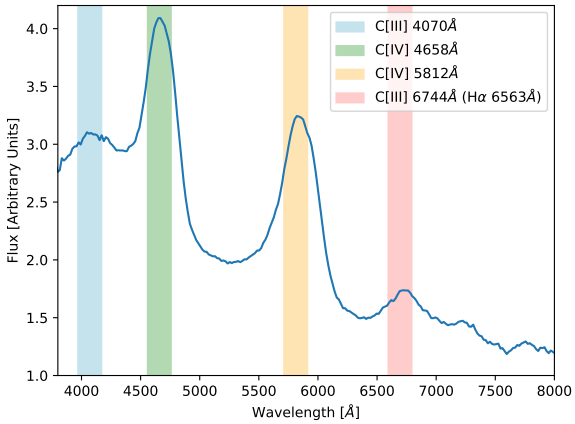

Figure 9. Calibrated spectrum of Wolf-Rayet star V1687 Cyg is shown in Figure 9. The spectrum is dominated by the emission lines of carbon, which is typical for a WC7 Wolf-Rayet star.

not accurate enough. If it is possible to fit a continuum to the spectrum, I can use the continuum-subtracted spectrum to locate the Balmer series more accurately, or even find them with gaussian fitting. However, since the sensitivity function is unknown in the wavelength calibration step, there is poor constraint on the continuum fitting. Maybe a better way is to calibrate using large number of standard stars with prominent Balmer absorption features, but this is not possible with the current data.

Another thing to note is that there seems to be a double peak in the Hβ absorption with an over 50Å gap, which is not intuitive in my current grasp of A0IV type stars. This could be a problem with the wavelength calibration, or the location of Balmer series. In practice, I just use the middle of the double peak as the location of Hβ, which is shown in Figure 5.

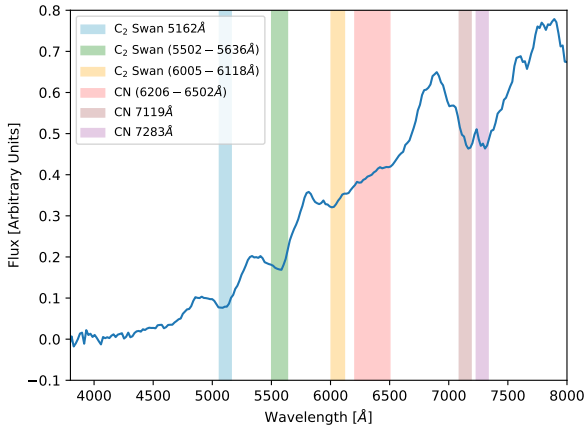

Figure 10. Calibrated spectrum of carbon star HK Lyr. The spectrum is dominated by the absorption features of carbon molecules, which is typical for carbon stars.

4.3. *Quantative Spectral Analysis*

The spectral type of carbon Wolf-Rayet star is partially determined by the ratio of C[III] emission to C[IV] emission. To carefully identify the spectral type of Wolf-Rayet star, I need to measure the flux ratio with the calibrated spectrum. However, the measurement of flux ratio is not included in the current pipeline yet. The following analysis will only be based on the qualitative features of the spectrum.

5. RESULTS

5.1. *Spectrum of Wolf-Rayet Star*

The calibrated spectrum of Wolf-Rayet star V1687 Cyg is shown in Figure 9. The spectrum is dominated by the emission lines of carbon, which is typical for a WC7 Wolf-Rayet star. The prominent emission in λ4658Å should be C[IV] 4658Å and another emission in λ5812Å is recognized as C[IV] 5812Å.

WC and WO spectra are formally distinguished based on the presence or absence of C[III] emission (Hucht 2001). The C[III] emission in 6744Å can be recognized to distinguish it from WO, though heavily blended with Hα emission in 6563Å.

The relatively weak C[III] emission in 6744Å indicates that the star can only be spectral type before WC8, and the spectral type before WC7 features negligible C[III] emission compared to C[IV] emission. This suggests that the spectral type of V1687 Cyg is WC7, which is consistent with Fahed et al. (2011).

5.2. *Spectrum of Carbon Star*

The calibrated spectrum of carbon star HK Lyr is shown in Figure 10.

As carbon stars are typically asymptotic giant branch (AGB) stars, they appear to be red in color, which is also consistent with the trend that the continuum of HK Lyr is expanding towards the red end of the spectrum.

The spectrum is dominated by features of carbon-containing molecules, such as CH, CN, and C_2, which is typical for carbon enhanced stars. In optical band, the most prominent features are the Swan band C_2 absorptions in λ5162Å, and complex series of Swan band absorptions in λ5502Å, λ5541Å, λ5585Å and λ5636Å.

Also, there is a platform (shown in yellow and red shaded area) possibly caused by another series of Swan band C_2 absorption: λ6005Å, λ6059Å, λ6122Å and λ6168Å. Right beside them are series of CN absorption: λ6206Å, λ6259Å, λ6355Å, and finally λ6502Å, contributing to the flattening as well.

An interesting W shape around λ7200Å can be explained by the absorption of two CN lines: λ7119Å and λ7283Å, represented in the maroon and purple shaded area in Figure 10.

Thank Professor Wang Ran for providing the data and some of the first stage reduction product.

Facilities: DoA Dome Telescope

Software: astropy (Astropy Collaboration et al. 2013), specutils (Earl et al. 2023), scikit-image (Van der Walt et al. 2014)

APPENDIX

A. OBSERVATION LOG

The observation log is shown in Table 1. The multiple exposures are coadded together to form a single image.

Table 1. Observation Log

Object	Filter	Exposure Time (s)	Number of Exposures	Date	Time Beijing
HK Lyr	CFW7	3.0	3	2023-10-10	21:10:03
HIP 90191	CFW7	0.5	3	2023-10-10	21:21:39
V1687 Cyg	CFW7	20	3	2023-10-10	21:59:41

REFERENCES

Astropy Collaboration, Robitaille, T. P., Tollerud, E. J., et al. 2013, A&A, 558, A33, doi: 10.1051/0004-6361/201322068

Earl, N., Tollerud, E., O'Steen, R., et al. 2023, astropy/specutils: v1.12.0, Zenodo, doi: 10.5281/zenodo.10016569

Fahed, R., Moffat, A. F. J., Zorec, J., et al. 2011, MNRAS, 418, 2, doi: 10.1111/j.1365-2966.2011.19035.x

Hucht, K. A. v. d. 2001, New Astronomy Reviews, 45, 135, doi: https://doi.org/10.1016/S1387-6473(00)00112-3

Van der Walt, S., Schönberger, J. L., Nunez-Iglesias, J., et al. 2014, PeerJ, 2, e453